Marine Chemistry 165 (2014) 10–24

Contents lists available at ScienceDirect

Marine Chemistry

journal homepage: www.elsevier.com/locate/marchem

Distribution, source and transportation of glycerol dialkyl glycerol tetraethers in surface sediments from the western Arctic Ocean and the northern Bering Sea

Yu-Hyeon Park [a,*], Masanobu Yamamoto [a,b], Seung-Il Nam [c], Tomohiro Irino [a,b], Leonid Polyak [d], Naomi Harada [e], Kana Nagashima [e], Boo-Keun Khim [f], Kazuhisa Chikita [g], Sei-Ichi Saitoh [h]

[a] Graduate School of Environmental Science, Hokkaido University, Kita-10, Nishi-5, Kita-ku, Sapporo 060-0810, Japan
[b] Faculty of Environmental Earth Science, Hokkaido University, Kita-10, Nishi-5, Kita-ku, Sapporo 060-0810, Japan
[c] Arctic Research Centre, Korea Polar Research Institute, 26-Songdomirae-ro, Yeonsu-gu, Incheon 406-840, Republic of Korea
[d] Byrd Polar Research Center, Ohio State University, Carmack Rd., Columbus, OH 43210, USA
[e] Research Institute for Global Change, Japan Agency for Marine-Earth Science and Technology, 2-15 Natsushimacho, Yokosuka 237-0061, Japan
[f] Department of Oceanography, Pusan National University, Busan 609-735, Republic of Korea
[g] Graduate School of Science, Hokkaido University, Kita-10, Nishi-8, Kita-ku, Sapporo 060-0810, Japan
[h] Faculty of Fisheries Sciences, Hokkaido University, 3-1-1 Minatocho, Hakodate 041-8661, Japan

ARTICLE INFO

Article history:
Received 14 November 2013
Received in revised form 26 June 2014
Accepted 3 July 2014
Available online 12 July 2014

Keywords:
GDGT
BIT
TEX_{86}
TEX^{L}_{86}
MBT′
CBT
Arctic Ocean
Chukchi Sea
Bering Sea

ABSTRACT

Isoprenoid and branched glycerol dialkyl glycerol tetraethers (GDGTs) and grain size distribution were investigated in surface sediments from the western Arctic Ocean including the Chukchi Sea and the adjacent northern Bering Sea to understand their source and transportation in the Arctic region and test environmental proxies derived from the GDGT composition.

Coarse sediments such as sand and silty sand are distributed in the Yukon and Mackenzie River estuaries, the northern Bering Sea near Bering Strait, and some areas of the outer shelf of the Bering Sea. In the Chukchi Sea, silt, grading from sandy to clayey silt, predominates and becomes finer northward towards the deep Arctic Ocean Isoprenoid GDGTs are abundant on the outer shelf and slope of the Chukchi Sea and the upper slope of the Bering Sea. The higher abundances are attributed to a combination of higher production of marine Archaea (Thaumarchaeota) at the shelf edge, redeposition of GDGT-carrying fine particles, and better preservation of GDGTs at sites with higher sedimentation rates. The TEX_{86}- and TEX^{L}_{86}-derived temperatures are not consistent with sea surface temperatures in the study area, with unrealistically high TEX_{86}- and TEX^{L}_{86}-derived temperatures in samples north of 73 °N probably biased by factors other than temperature.

Branched GDGTs are abundant on the Chukchi shelf and in the Yukon and Mackenzie River estuaries. At the shelf edge of the Chukchi Sea, both branched and isoprenoid GDGTs are abundant, indicating common concentration processes such as sediment redeposition and efficient preservation at sites with high sedimentation rates. Sediments from the western Arctic Ocean north of 75 °N, the Yukon and Mackenzie River estuaries, and the Yukon River have higher cyclization ratio of branched tetraethers (CBT) than sediments from the Chukchi and Bering Seas, suggesting two different sources of branched GDGTs inferred as soil and marine bacteria.

1. Introduction

As global warming continues and the extent of Arctic sea ice decreases rapidly, the Arctic Ocean is experiencing a dramatic environmental change. Furthermore, strong positive feedbacks in the Arctic climate system may affect the global climate (Miller et al., 2010; Screen and Simmonds, 2010). Paleoclimate studies are important to better understand ongoing change in the Arctic. As paleoclimate proxies applicable to Arctic sedimentary records are limited because of sparse occurrence of microfossils and severe alteration of chemical compositions, development and tests of new proxies are much needed for accurate paleoclimate investigation of the Arctic Ocean.

Glycerol dialkyl glycerol tetraethers (GDGTs) have been introduced as a proxy to trace environmental changes by estimating the contribution of soil organic matter (Hopmans et al., 2004; Sinninghe Damsté et al., 2000), sea surface temperature (Schouten et al., 2002), soil pH and mean annual air temperature in the provenance areas (Peterse et al., 2012; Weijers et al., 2007). GDGTs were used for reconstruction the late Quaternary environment in the Arctic Ocean (Faux et al., 2011; Yamamoto et al., 2008; Yamamoto and Polyak, 2009). However, the applicability of GDGT proxies is not yet established because GDGT

* Corresponding author.
E-mail address: parkyh@ees.hokudai.ac.jp (Y.-H. Park).

http://dx.doi.org/10.1016/j.marchem.2014.07.001
0304-4203/

compositions are not simply correlated with surface water condition in the Arctic Ocean, in contrast to other oceans in the mid- and low-latitudes, suggesting that non-temperature factors such as depositional environment might influence GDGT compositions (Ho et al., 2014; Kim et al., 2010, 2012; Liu et al., 2009). In this study, we report the first investigation of GDGTs from surface sediments collected from the Chukchi region of the western Arctic including the Chukchi Sea and adjacent areas of the deep Arctic Ocean and the Bering Sea. The study is aimed to understand the sources, transportation, and deposition patterns of isoprenoid and branched GDGTs in the Arctic and to test the proxies derived from the GDGT composition.

2. Background information

2.1. Study area

The western or Amerasian part of the Arctic Ocean is separated by the submarine Lomonosov Ridge from the eastern Arctic Ocean and is bound by the coasts of eastern Siberia, Alaska, and Canadian Arctic, with a limited connection to the Pacific Ocean via a narrow Bering Strait. Oceanographic processes in the western Arctic are strongly affected by high fluxes of riverine waters and more hydrographic isolation due to the Beaufort Gyre circulation system and limited deep water exchange with Atlantic Ocean water by Lomonosov Ridge (Polyak et al., 2009). These features largely control the distribution of water masses and associated dissolved and suspended matter in the western Arctic Ocean (e.g. Bates et al., 2011; Codispoti et al., 2005; Giles et al., 2012; Macdonald et al., 2002). The Chukchi Sea encompasses a broad, shallow, and extensively ice covered continental shelf between the eastern Siberia and Alaska. To the south it is connected to the Bering Sea via the narrow and shallow Bering Strait, and to the north the Chukchi shelf borders the deep Arctic Ocean, with a system of submarine ridges and plateaus extending from the shelf. Sea ice extent and primary productivity in the Chukchi Sea show strong seasonal variation. During summer, the retreat of sea ice margin across the Chukchi shelf causes high primary production and surface water stratification (Cota et al., 1996; Hill and Cota, 2005). Stronger ice cover further north controls the decreasing northward pattern in temperature and salinity in the surface layer. Hydrography and sea ice distribution are also strongly affected by the Pacific waters entering through the Bering Strait (e.g., Shimada et al., 2006; Weingartner et al., 2005; Woodgate and Aagaard, 2005; Woodgate et al., 2005a, 2005b). In addition to major currents, local hydrological features such as diapycnal mixing (Pickart et al., 2005), eddies (Pickart, 2004), density flow from ice formation (Williams et al., 2008) and upwelling (Woodgate et al., 2005a) are important for transport of water and sediments in the Chukchi region.

Sediment is primarily delivered to the Chukchi Sea by the discharge of local rivers, coastal erosion, and the Bering Strait inflow, and redistributed on the shelf by bottom erosion and redeposition (e.g., Darby et al., 2009; Viscosi-Shirley et al., 2003). Sea ice also plays an important role in sediment transport from the Siberian and North American margins (Darby, 2003; Darby et al., 2009). Investigation of inorganic and organic sedimentary proxies in the Chukchi Sea and adjacent Arctic Ocean provides valuable information for understanding both recent and longer-term Arctic environmental changes (e.g., Belicka et al., 2002; Belicka and Harvey, 2009; Darby et al., 2009; Faux et al., 2011; Polyak et al., 2009; Viscosi-Shirley et al., 2003; Yamamoto et al., 2008; Yamamoto and Polyak, 2009; Yunker et al., 1993; 2011; Yurco et al., 2010). Sampling stations are grouped by water depth broadly corresponding to inner shelf (0–50 m), outer shelf (50–140 m), slope (140–2000 m) and basin (>2000 m) (Fig. 1).

2.2. GDGT proxies

Isoprenoid GDGTs are produced by marine Archaea and ubiquitously found in marine environments (Sinninghe Damsté et al., 2002). The pattern of relative abundance of GDGT-0 to GDGT-3 and crenarchaeol in marine sediments, except for estuarine areas, indicates that isoprenoid GDGTs are mainly produced by Thaumarchaeota, formerly classified as Crenarchaeota marine group I (Sinninghe Damsté et al., 2002; Spang et al., 2010). Thaumarchaeota are chemoautrophic nitrifiers (e.g., Alonso-Sáez et al., 2012; Hallam et al., 2006; Könneke et al., 2005; Wuchter et al., 2006) and heterotrophs (e.g., Agogué et al., 2008; Ouverney and Fuhrman, 2000; Zhang et al., 2009) and are common in cold marine waters (DeLong et al., 1994; Wuchter et al., 2006). Several reports confirm the existence of Thaumarchaeota in the Arctic Ocean (Alonso-Sáez et al., 2008; 2012; Amano-Sato et al., 2013; Bano et al., 2004; Kirchman et al., 2007). In the Chukchi Sea, Thaumarchaeota abundance shows spatial and seasonal variations, correlated with nitrate, phosphate and ammonia concentrations (Kirchman et al., 2007).

TEX_{86}, the index based on the composition of isoprenoid GDGTs, was proposed as a proxy for temperature proxy of overlaying sea surface water (Schouten et al., 2002). TEX^{L}_{86}, proposed by Kim et al. (2010), is modified from TEX_{86} based on more extensive core-top dataset from polar and subpolar oceans. Recently, Kim et al. (2012) suggested that the calibration of TEX^{L}_{86} to integrated temperatures between 0 and 200 m is better than the calibration to SST in the application in the polar oceans. However, substantial scatter in TEX_{86}/TEX^{L}_{86} and temperature in the low-temperature range suggests that factors other than temperature influence the TEX_{86}/TEX^{L}_{86} in the cold water regions.

Methane index based on the composition of isoprenoid GDGTs, which could be contributed by methane oxidizing Archaea, was proposed as a proxy for the anaerobic oxidation of methane by Euryarchaeota (Zhang et al., 2011). TEX_{86} is biased when the contribution of Euryarchaeota is large (methane index > 0.4).

Branched GDGTs are commonly found in soils (Hopmans et al., 2004) and thought to be produced by Acidobacteria (Sinninghe Damsté et al., 2011). Although the production of branched GDGTs in the lacustrine environments has been speculated in several studies (e.g., Blaga et al., 2009; Sinninghe Damsté et al., 2009; Tierney and Russell, 2009), overall branched GDGTs are robust tracers of organic matter from terrestrial soils in marine environments (Hopmans et al., 2004). MBT and CBT indices (methylation index and cyclization ratio of branched tetraethers) based on the composition of branched GDGTs were proposed as proxies of soil pH and mean annual air temperature at provenance sites (Weijers et al., 2007). These indices are thus useful for identification of the source areas of organic matter.

Branched and isoprenoid tetraether (BIT) index is defined as the ratio of branched GDGTs to the sum of branched GDGTs and crenarchaeol (Hopmans et al., 2004). The index is used as a proxy of soil organic matter contribution. However, at higher latitudes in situ production of branched GDGTs was also inferred for marine environments (Peterse et al., 2009).

3. Materials and methods

3.1. Samples

A total of 78 core-top (0–0.5 or 0–1 cm depth) sediment samples were collected in the Chukchi Sea and the adjacent Arctic Ocean, the northern Bering Sea, and the Yukon and Mackenzie River estuaries using a multiple corer and/or gravity corer during 2000 to 2013 from RV Araon (ARA01B and 02B), RV Mirai (MR00 and MR06 cruises) and T/S Oshoro-maru (Fig. 1). In addition, sediments were sampled from the Yukon River using an Ekman-Birge grab sampler (Fig. 1B). Samples were stored in a refrigerator on board and freeze dried in the laboratory.

3.2. Analytical methods

3.2.1. Grain size analysis

Approximately 100 mg of bulk sediment was analyzed with a laser diffraction scattering grain size analyzer (Horiba LA-920) after 10%

hexametaphosphate treatment to disperse particles following a method of Nagashima et al. (2012). Grain size was classified in a 0.02 to 2000 μm diameter range with a Δlog10 (μm) = 0.06 interval and was expressed as volume percent (%). Using the Igor pro software, the distribution of grain size was separated into several peaks by curve fitting to determine the clay, silt and sand volume contents. Reproducibility was better than 2% for each grain size interval (Nagashima et al., 2012).

3.2.2. GDGT analysis

Lipids were extracted from dried and homogenized sediment (1–3 g) with 11 ml of mixture of dichloromethane:methanol (6:4 v:v) at 100 °C and 1000 psi for 10 min three times using a DIONEX accelerated solvent extractor (ASE-200) and then concentrated using a rotary evaporator. The extract was separated into four fractions according to the degree of polarity, F1 (3 ml hexane), F2 (3 ml of hexane:toluene

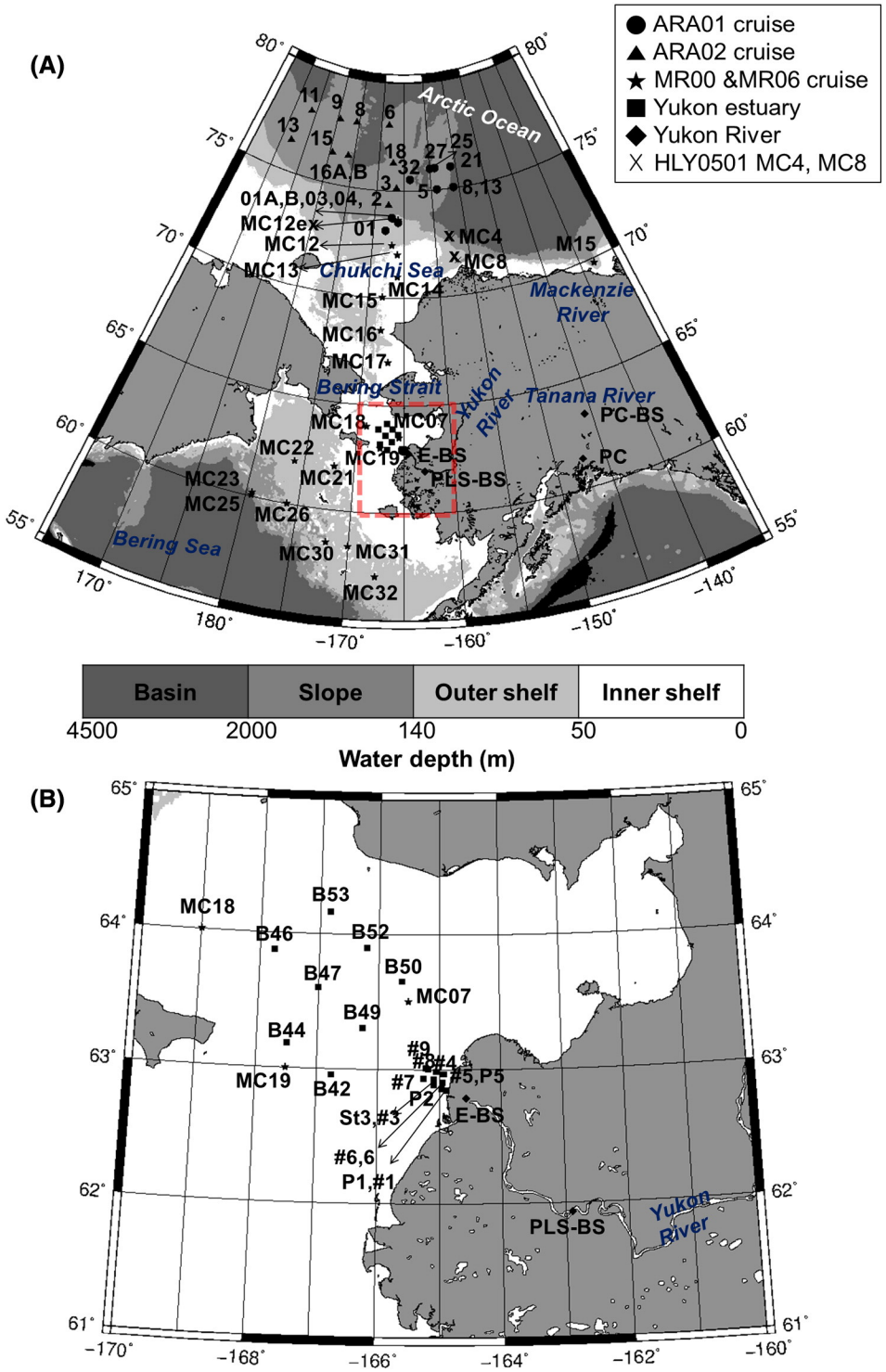

Fig. 1. Map showing the locations of (A) surface sediment samples in the western Arctic Ocean, the Chukchi Sea, the Bering Sea, and (B) the Yukon River estuary.

(3:1 v:v)), F3 (4 ml of toluene) and F4 (3 ml of toluene:methanol (3:1 v:v)), using column chromatography (silica gel with 5% distilled water, i.d.: 5.5 mm, length: 45 mm). For GDGT analysis, F4 fraction was dissolved in hexane-2-propanol (99:1 v:v), and then filtered using an sodium sulfate column. After adding an internal standard (C_{46} GTGT; Patwardhan and Thompson, 1999), GDGTs were analyzed by high performance liquid chromatography–mass spectrometry (HPLC–MS) with a Shimadzu HPLC system connected to a Bruker Daltonics micrOTOF-HS time-of-flight mass spectrometer. Separation in HPLC was conducted using a Prevail Cyano column (2.1 × 150 mm, 3 μm) from Alltech and maintained at 30 °C following the methods of Hopmans et al. (2000) and Schouten et al. (2007). The condition of liquid chromatograph was 0.2 ml/min flow rate, isocratic with 99% and 1% 2-propanol for the first 5 min followed by linear gradient to 1.8% 2-propanol over 45 min. Ionization was carried out using an atmospheric pressure, positive ion chemical ionization method. Detection of ions was processed in the full scan mode (m/z 500–1500). GDGTs were identified by comparing their mass spectra and the retention times with those published in Hopmans et al (2000) and quantified by comparing the summed peak areas in the $(M + H)^+$ and the isotopic $(M + H + 1)^+$ ion to the peak area of internal standard (Huguet et al., 2006). Chemical structures of the investigated GDGTs are shown in the Appendix A.

TEX_{86} was calculated from concentrations of GDGT-1, GDGT-2, GDGT-3 and crenarchaeol regioisomer using the following expression (Schouten et al., 2002):

$$TEX_{86} = ([GDGT-2] + [GDGT-3] + [\text{crenarchaeol regioisomer}]) / ([GDGT-1] + [GDGT-2] + [GDGT-3] + [\text{crenarchaeol regioisomer}]).$$

TEX_{86}-derived temperature was calculated according to the following equation based on a global core-top calibration (Kim et al., 2010):

$$T = 81.5\ TEX_{86} - 26.6,$$

where T = temperature (°C). The standard deviations of five duplicate analyses for F4 fractions averaged 1.2 °C.

TEX_{86}^L, modified TEX_{86}, was calculated from the concentrations of GDGT-1, GDGT-2 and GDGT-3 using the following expression (Kim et al., 2010):

$$TEX_{86}^L = \log\{[GDGT-2]/([GDGT-1] + [GDGT-2] + [GDGT-3])\}.$$

TEX_{86}^L-derived temperature was calculated according to the following equation based on a global core-top calibration (Kim et al., 2010):

$$T = 67.5\ TEX_{86}^L + 46.9,$$

where T = temperature (°C), The standard deviations of 5 duplicate analyses for fraction averaged 2.1 °C.

Methane index (MI) was calculated from the concentrations of GDGT-1, GDGT-2, GDGT-3, crenarchaeol, and crenarchaeol regioisomer using the following expression (Zhang et al., 2011):

$$MI = ([GDGT-1] + [GDGT-2] + [GDGT-3]) / ([GDGT-1] + [GDGT-2] + [GDGT-3] + [\text{crenarchaeol}] + [\text{crenarchaeol regioisomer}]).$$

Branched and isoprenoid tetraether (BIT) index was calculated from the concentrations of GDGT-I (I), GDGT-II (II), GDGT-III (III) and crenarchaeol using the following expression (Hopmans et al., 2004):

$$BIT = ([I] + [II] + [III]) / ([I] + [II] + [III] + [\text{crenarchaeol}]).$$

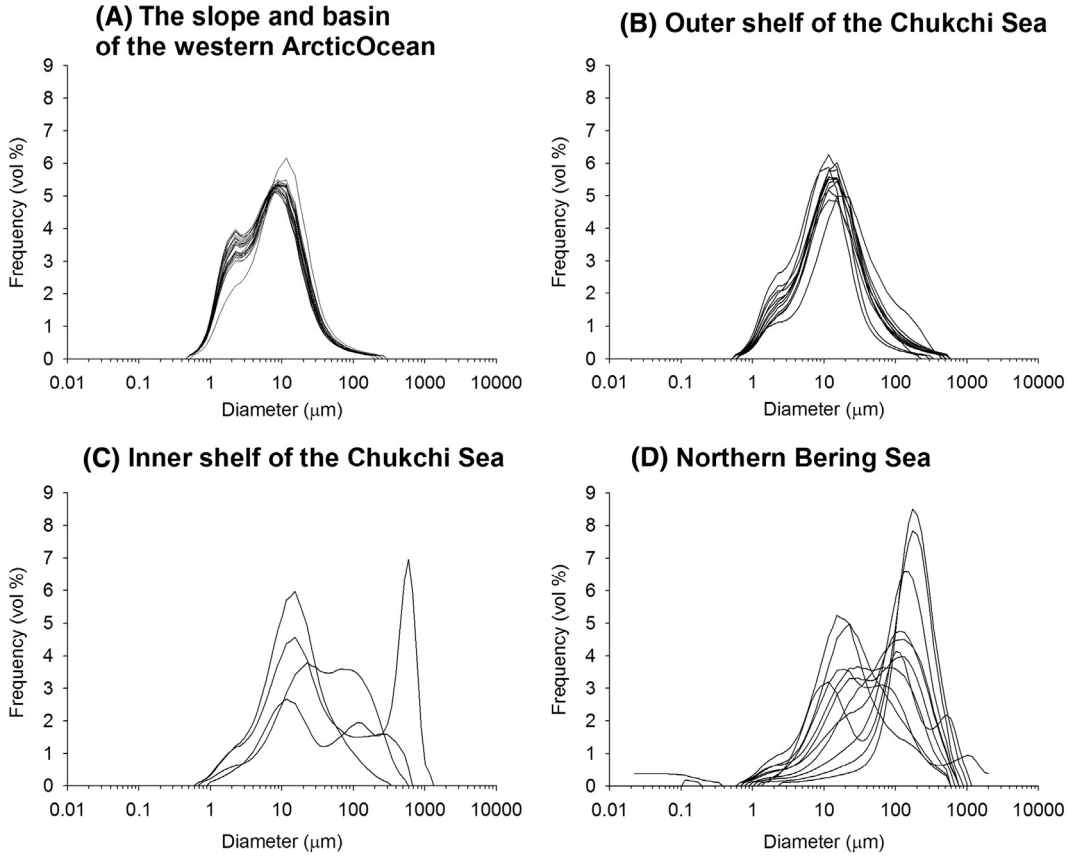

Fig. 2. Grain size distributions of surface sediments in (A) the slope and basin of the western Arctic Ocean, (B) outer shelf of the Chukchi Sea, (C) inner shelf of the Chukchi Sea, and (D) northern Bering Sea.

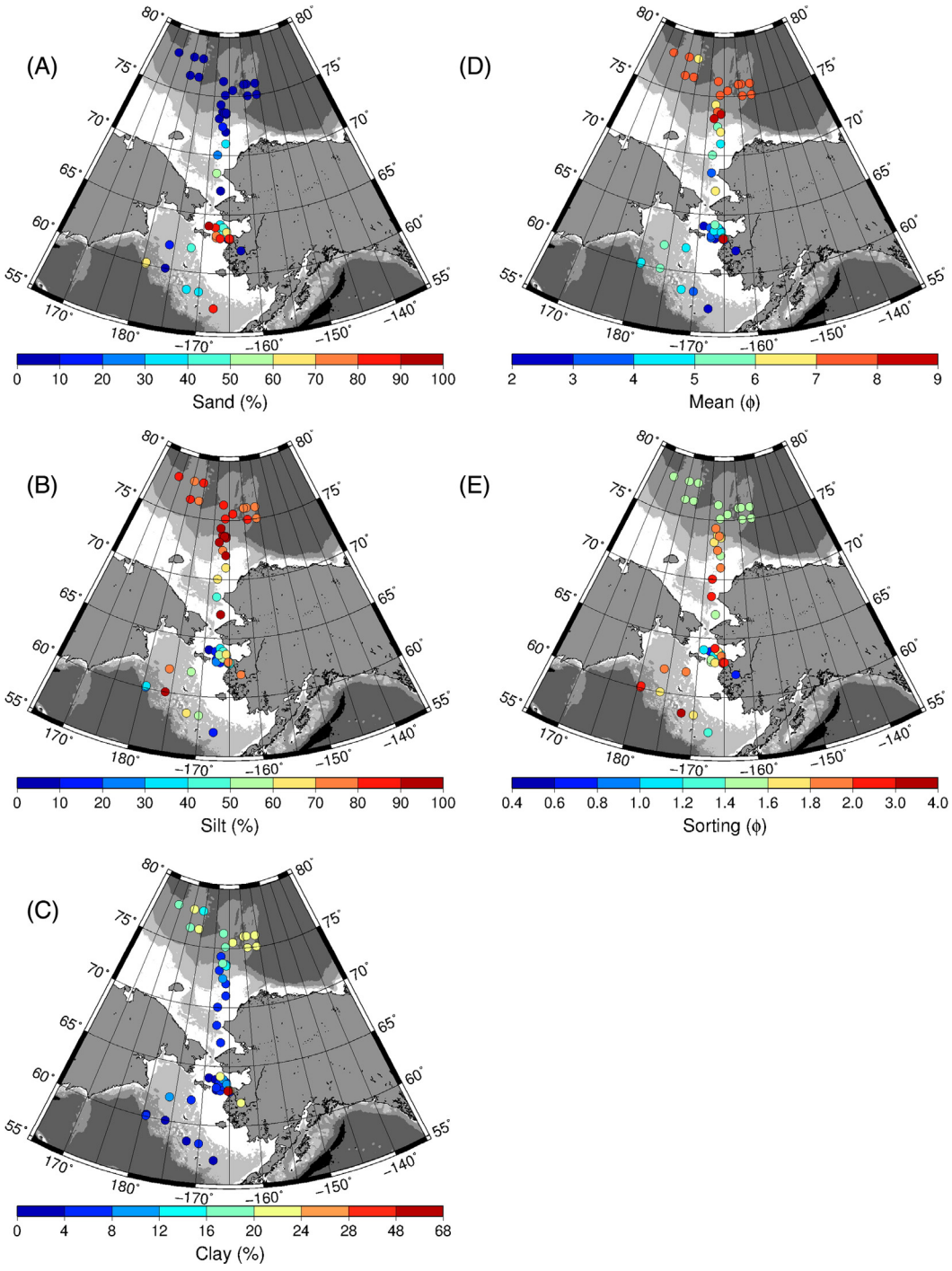

Fig. 3. The contents of (A) sand, (B) silt, (C) clay, (D) mean grain size and (E) sorting in the western Arctic Ocean, the Chukchi Sea, and the northern Bering Sea.

The cyclization ratio of branched tetraethers (CBT) was calculated from the concentrations of GDGT-I (I), GDGT-Ib (Ib), GDGT-II (II), and GDGT-IIb (IIb) using the following expression (Weijers et al., 2007):

$$CBT = -\log\{([Ib] + [IIb])/([I] + [II])\}.$$

Soil pH was calculated according to the following equation based on a global soil calibration (Peterse et al., 2012; Weijers et al., 2007):

$$pH = 7.90 - 1.97\ CBT.$$

The methylation index of branched tetraethers (MBT′) was calculated from the concentrations of branched GDGTs shown in the Appendix A using the following expression (Peterse et al., 2012). Roman numerals in the expression refer to the abbreviations in Appendix A:

$$MBT\prime = ([I] + [Ib] + [Ic])/([I] + [Ib] + [Ic] + [II] + [IIb] + [IIc] + [III]).$$

Mean annual air temperature (MAAT) was calculated from the MBT′ and CBT indices according to the following equation based on a global soil calibration (Peterse et al., 2012):

$$MAAT = 0.81 - 5.67\ CBT + 31.0\ MBT\prime.$$

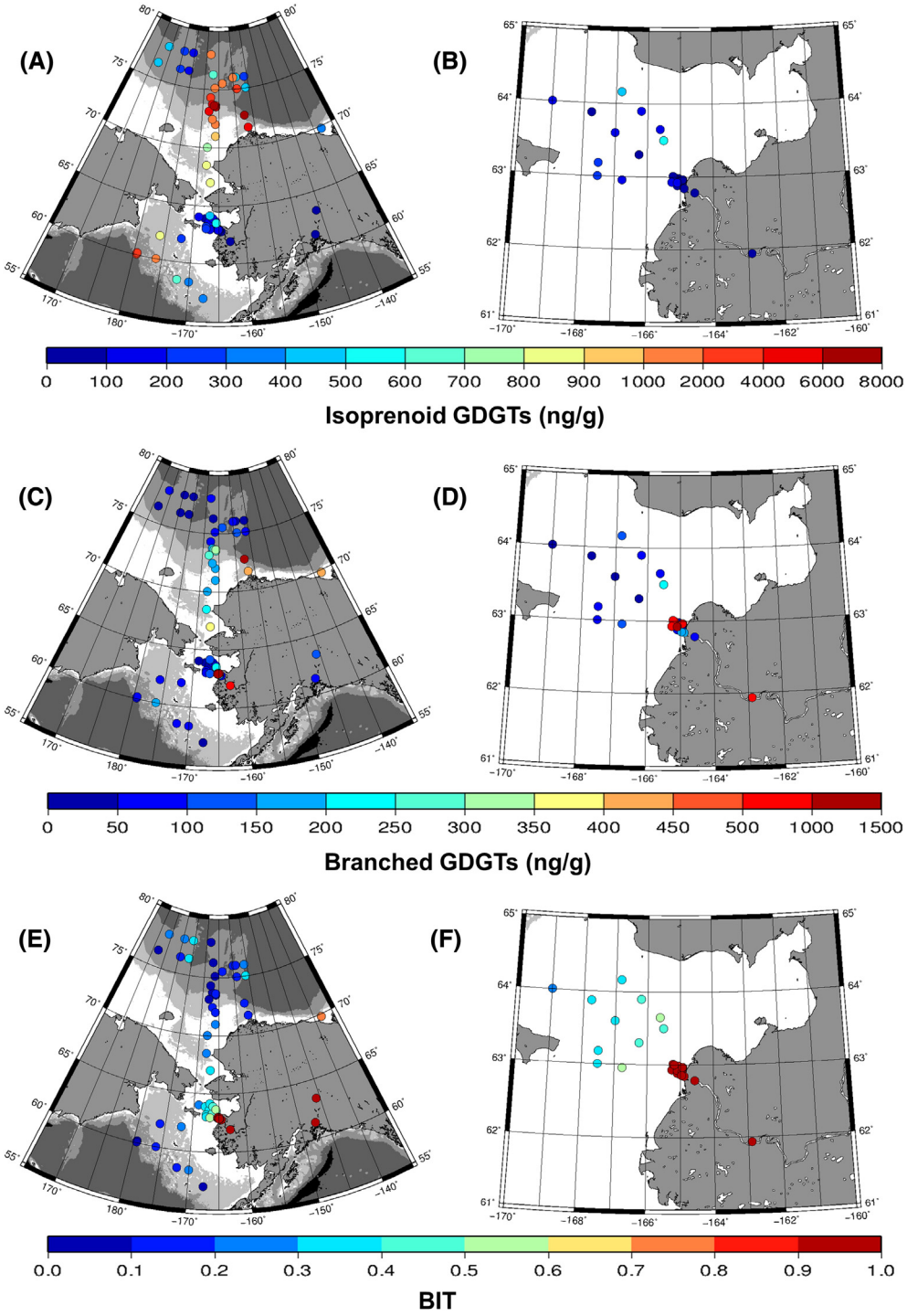

Fig. 4. Concentrations of (A and B) isoprenoid GDGTs and (C and D) branched GDGTs, (E and F) BIT indices, (G and H) ratio of caldarchaeol to crenarchaeol (Cald/Cren), (I and J) methane index, (K and L) TEX_{86}^{L}-derived temperature, (M and N) CBT, (O and P) MBT′ and (Q and R) MAAT in the western Arctic Ocean, the Chukchi Sea, and the northern Bering Sea.

4. Results

4.1. Grain size

Analyzed surface sediments consist mainly of sandy silt in the Bering Sea, the Yukon River estuary and the inner shelf of the Chukchi Sea, pure fine silt on the outer Chukchi shelf, and clayey silt in the western Arctic Ocean north of 75 °N (Fig. 2). Grain size distribution in the Chukchi Sea region shows a bimodal distribution of silt and clay in the Arctic Ocean off the shelf (Fig. 2A), a unimodal distribution with a shoulder of clay on the outer Chukchi shelf (Fig. 2B), and a bimodal distribution of silt and fine sand with a shoulder of clay on the inner Chukchi shelf (Fig. 2C). Sediments from the Bering Sea and the Yukon River estuary show variable multimodal patterns of silt and sand (Fig. 2D; Nagashima et al., 2012). Sand is most abundant in the Bering Sea and the inner Chukchi shelf, silt is common in the Arctic Ocean, outer Chukchi shelf and some sites of the outer Bering shelf, and clay is abundant in the Arctic Ocean (Fig. 3A–C). Mean grain size ranges from 5.8 μm to 300 μm and is generally higher in the Bering Sea and on the inner Chukchi shelf than further north (Fig. 3D). Sorting is better in the Arctic Ocean off the shelf than in the Chukchi and Bering shelf areas (Fig. 3E). In the Yukon River estuary and the Yukon–Tanana River sediments, the

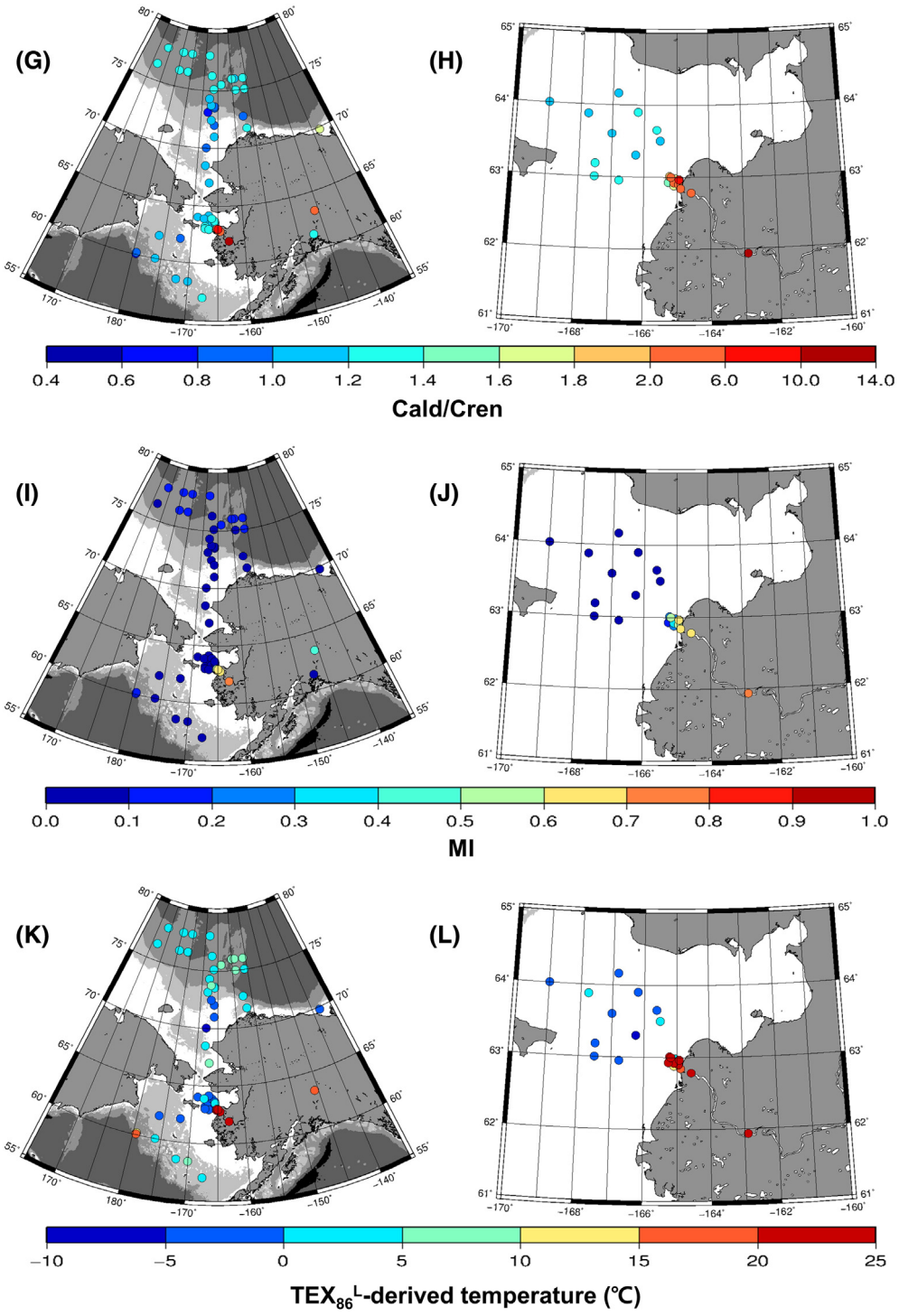

Fig. 4 (*continued*).

mean grain size (5.8–160 μm) is generally larger than on the outer Chukchi shelf.

4.2. GDGTs

A total of 15 GDGTs shown in the Appendix A, which are all compounds used for TEX_{86}, TEX_{86}^{L} and MBT′/CBT proxies, were detected in sediment samples (Fig. 4). The concentrations of isoprenoid and branched GDGTs range from 2 to 7630 ng/l and from 14 to 1494 ng/l, respectively. Isoprenoid GDGTs are most abundant on the outer Chukchi shelf including the north Alaska margin (MC04 and MC08) and on the continental slope of the northwestern Bering Sea (MC23, MC25 and MC26) (Fig. 4A and B). Concentrations of isoprenoid GDGTs in the Yukon River estuary and Yukon–Tanana River sediments are lower than in other areas (Fig. 4A and B). In contrast, branched GDGTs are more abundant in the Mackenzie and Yukon River estuaries, as well as on the Chukchi shelf, than in the Arctic Ocean off the shelf and the Bering Sea (Fig. 4C). Concentrations of branched GDGTs in the Yukon River estuary sediments are high but decrease rapidly offshore within an 80 km distance (Fig. 4D). Sediment from the downstream of the

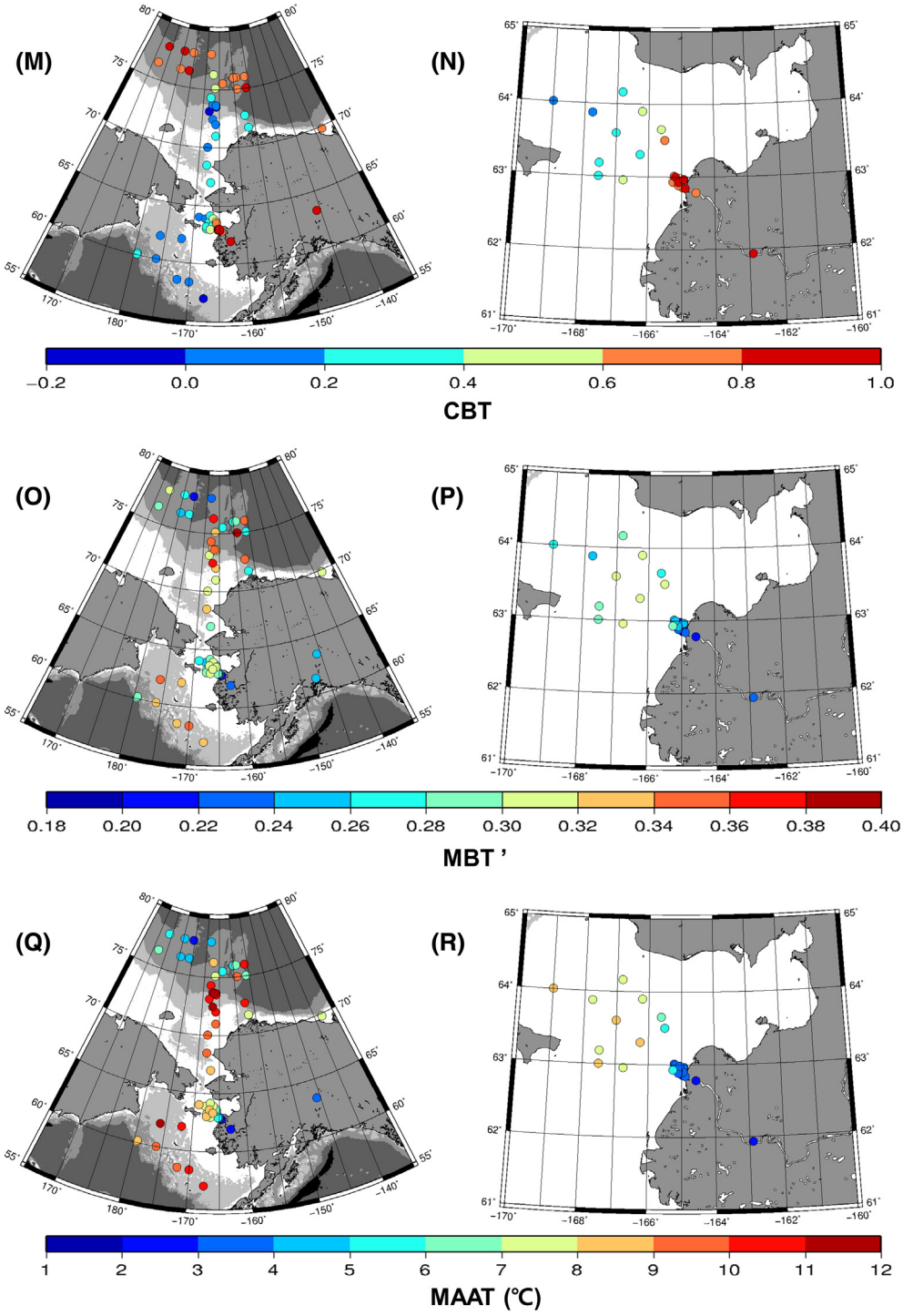

Fig. 4 (*continued*).

Yukon River shows the highest concentration of branched GDGTs (Fig. 4C). The BIT index (Hopmans et al., 2004), ranging from 0.03 to 0.99, is highest in the Yukon and Mackenzie River estuaries. In the Chukchi Sea, BIT values, ranging from 0.03 to 0.39, decreases northward to 75 °N, but some samples (13 and 21 sites in ARA01 cruise, and 8, 9, 11, 16A and 16B sites in ARA02 cruise) further north of 75 °N show higher BIT values (0.23 to 0.39) than other sites in the Chukchi Sea (Fig. 4E). In the Bering Sea BIT decreases rapidly with the distance from the Yukon River estuary (Fig. 4F), and high BIT values of ~0.99 in the Yukon–Tanana River sediments are typical for terrestrial soils (Fig. 4E).

The ratio of caldarchaeol (GDGT-0) to crenarchaeol (Cald/Cren), ranging from 0.5 to 13.2, is high in the Yukon and Mackenzie River estuaries and lowest on the upper slope north of the Chukchi shelf (Fig. 4G and H). Methane Index (MI) values (Zhang et al., 2011), ranging from 0 to 0.74, are low in most stations, but high in the Yukon River estuary and Yukon–Tanana River sediments (Fig. 4I and J). Generated TEX_{86}- and TEX^{L}_{86}-derived temperatures range from −9.7 to 24.7 °C and show no agreement with either annual or summer climatological sea surface temperatures (SSTs) (Fig. 5). In the Bering Sea and the southern Chukchi Sea, the TEX_{86}- and TEX^{L}_{86}-derived temperatures are lower than

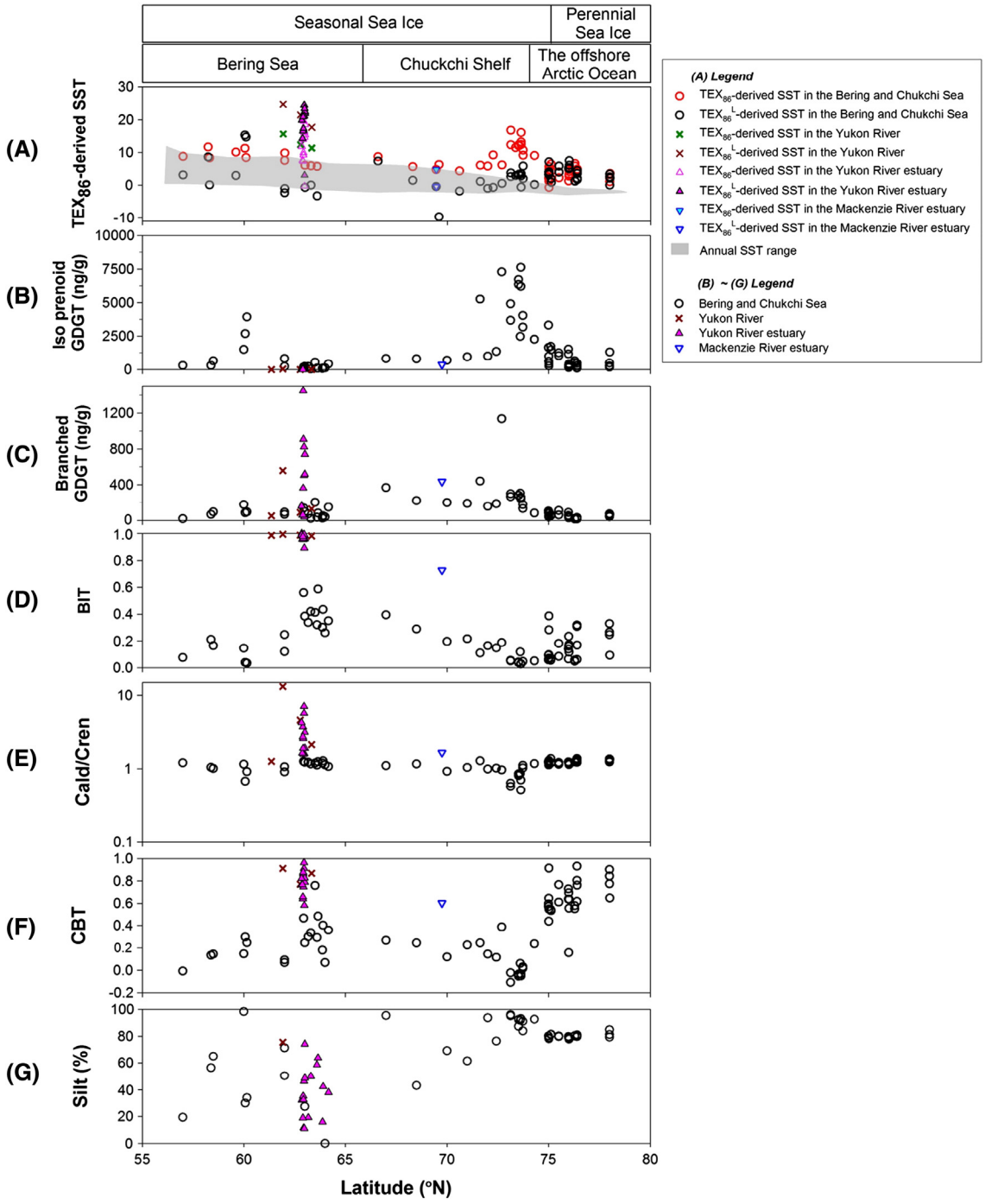

Fig. 5. (A) TEX_{86}- and TEX_{86}^{L}-derived temperatures, annual SST range, (B and C) concentrations of isoprenoid and branched GDGTs, (D) BIT, (E) Cald/Cren, (F) CBT and (G) silt content along the latitudinal transect from the Bering Sea to the Arctic Ocean. Climatological SST data are from the World Ocean Atlas, 2009. Sea ice data is from National Snow and Ice Data Center (September median during 1979–2000).

SSTs at some sites and higher at other sites (Fig. 5). In the area north of 73 °N the TEX_{86}- and TEX_{86}^{L}-derived temperatures are consistently higher than the SSTs (Fig. 5). In the Yukon River estuary and Yukon–Tanana River sediments, TEX_{86}- and TEX_{86}^{L}-derived temperatures are much higher than the SSTs (Fig. 4K and L).

CBT index ranges from −0.11 to 0.96 with higher values in the Arctic Ocean and the Yukon and Mackenzie River estuaries than on the Chukchi and Bering Sea shelves (Fig. 4M and N). MBT′ index ranges from 0.19 to 0.38 and is generally higher on the Chukchi and Bering shelves (Fig. 4O and P). MBT′/CBT-based MAAT ranged from −4.8 to 9.9 °C with high values in the Chukchi and Bering shelves (Fig. 4Q and R). The Yukon River estuary and the Yukon–Tanana River sediments have higher CBT, lower MBT′ and lower MBT′/CBT-based MAAT values than in the northern Bering Sea further offshore (Fig. 4N, P and R).

5. Discussion

5.1. Sources and transportation of sediments

Our results indicate that coarse sediments such as sand and silty sand are distributed in the Yukon and Mackenzie River estuaries, the northern Bering Sea near Bering Strait, and some areas of the outer

shelf of the Bering Sea (Fig. 3A). In the Chukchi Sea, silt, grading from sandy to clayey silt, predominates and becomes finer northward towards the deep Arctic Ocean (Fig. 3B and C).

Sediment is largely supplied to the study area by rivers and coastal erosion that is active along the adjacent coasts (Harper, 1978). The Yukon River, one of the major world rivers discharging high sediment load (Brabets et al., 2000), supplies detrital particles to the Bering Sea. The distribution of clay minerals in the Chukchi Sea sediments suggested that particles can be transported from the Bering to the Chukchi Sea via the Bering Strait (Kalinenko, 2001; Ortiz et al., 2009). In addition, multiple small rivers discharge sediment to the Chukchi and Bering seas (Gordeev, 2006; Holmes et al., 2002; Macdonald et al., 2002; Nagashima et al., 2012). Another potential sediment source is the resuspension of finer particles in high-energy environments on the inner shelf (Are, 1996; Stein et al., 2004). Resuspended particles are advected by water currents and deposited in lower energy environments on the slope and adjacent deep basins, thus focusing finer sediments in these areas (Darby et al., 2009).

The silt content is maximal and sorting is good around the shelf edge of the Chukchi Sea about 73 °N (Figs. 3B, E and 5). Sediments change noticeably further north, where clay content gets higher and sorting is better, especially north of 75 °N. The boundary between clayey silt and pure fine silt corresponds to the average position of summer sea ice margin in the 20th century (Data from National Snow and Ice Data Center http://nsidc.org/data/seaice_index/). This correspondence suggests that ice distribution controls depositional processes and, thus, the difference in lithology between the two areas. This control may be related to the blockage of Bering Strait originating surface currents north of 75 °N and the transport of sediment by sea ice. Sediments carried by ice drift may have a wide grain size spectrum from clay to gravel (Stein et al., 1994), but in the Arctic Ocean they are mostly composed of fine particles (Polyak et al., 2010, and references therein). In addition to sea ice transport, Darby et al. (2009) concluded that nepheloid flows provide a major transport mechanism of sorted clay and fine silt from the inner Chukchi shelf to the slope of the Chukchi–Alaskan margin. We infer that sediments north of 75 °N are deposited by a combination of well sorted fine silt derived from the inner Chukchi shelf and the East Siberian shelf by currents and clay and fine silt particles carried by sea ice from the North American margin via the Beaufort Gyre circulation.

5.2. Sources of isoprenoid GDGTs in the western Arctic

Isoprenoid GDGTs are specific to Archaea (Nishihara and Koga, 1987). Thaumarchaeota are dominant Archaea, while Euryarchaeota are less abundant in the water column in the Chukchi and Bering Seas (Amano-Sato et al., 2013; Kirchman et al., 2007). Crenarchaeol, specific to Thaumarchaeota (Sinninghe Damsté et al., 2002), is common in the study samples, suggesting that Thaumarchaeota are a dominant source of isoprenoid GDGTs in the study area. The distribution of isoprenoid GDGTs is spatially variable across the study area, with the highest abundance found on the outer shelf and some sites in the slope of the Chukchi Sea and the upper slope of the Bering Sea (Figs. 4A and 5). In the Chukchi and Bering seas primary production is spatially variable and sporadic (Belicka and Harvey, 2009; Cota et al., 1996; Grebmeier et al., 2006; Wang et al., 2005). As chemoautrophic nitrifiers and heterotrophs, Thaumarchaeota need ammonia, urea or organic matter as an energy source. Low marine production in waters covered by perennial sea ice (Arrigo et al., 2008; Lee et al., 2010; Wang et al., 2005) results in low concentrations of ammonia, urea and organic matter in the water column and potentially accounts for a low concentration of GDGTs in the area north of 75 °N. High isoprenoid GDGT concentrations on the outer shelf and upper slope of the Chukchi Sea is associated with a low ratio of Cald/Cren (0.51–1.17; Figs. 4A, G and 5). Because crenarchaeol is specific to Thaumarchaeota (Sinninghe Damsté et al., 2002) and caldarchaeol is common in most Archaea (e.g., Schouten et al., 2013), the low Cald/Cren ratio suggests that the enhanced production of Thaumarchaeota on the outer shelf and upper slope contributes to abundant isoprenoid GDGTs. High concentrations of isoprenoid GDGTs in this area are found in sediments with well sorted silt fraction (Fig. 5), suggesting redeposition of fine particles with higher GDGT concentration. Also, high sedimentation rates in this area (>50 cm/kyr; Darby et al., 2009; Polyak et al., 2009) enhance the preservation of isoprenoid GDGTs by allowing them to escape from microbial degradation within relatively short time. We thus attribute the high concentration of isoprenoid GDGTs on the outer shelf and upper slope of the Chukchi Sea to a combination of the enhanced production of Thaumarchaeota, accumulation of isoprenoid GDGTs associated with advected fine particles, and the efficient preservation by rapid deposition (Table 1).

Table 1
Summary of the potential source of GDGTs in surface sediments from the western Arctic Ocean, the Chukchi Sea, the Bering Sea, the Yukon and Mackenzie River estuaries, and the Yukon–Tanana River sediments.

Locations	Sediments	GDGTs	Possible major archaeal GDGT source	Possible major bacterial GDGT source
Western Arctic Ocean north of 75 °N	Silt and clay	Low to high isoprenoid and low branched GDGT concentrations, moderate BIT, Higher TEX_{86} and TEX^{L}_{86} than SST, Low Cald/Cren, Low MI, High CBT	Thaumarchaeota produced in situ	Soil bacteria
Outer shelf of the Chukchi Sea 73–75 °N	Silt and minor clay	High isoprenoid and high branched GDGT concentrations, Low BIT, Higher TEX_{86} and TEX^{L}_{86} than SST, Low Cald/Cren, Low MI, low CBT	Thaumarchaeota produced in situ	Bacteria in marine environments
Inner shelf of the Chukchi Sea 66–73 °N	Silt and sand	Moderate isoprenoid and high branched GDGT concentrations, Moderate BIT, Moderate TEX_{86} and TEX^{L}_{86}, Low Cald/Cren, Low MI, low CBT	Thaumarchaeota produced in situ	Bacteria in marine environments
Offshore Bering Sea	Silt and sand	Low to high isoprenoid and low branched GDGT concentrations, Moderate BIT, Moderate TEX_{86} and TEX^{L}_{86}, Low Cald/Cren, Low MI, low CBT	Thaumarchaeota produced in situ	Bacteria in marine environments
The Yukon River estuary	Sand and silt	Low isoprenoid and high branched GDGT concentrations, High BIT, High TEX_{86} and TEX^{L}_{86}, High Cald/Cren, High MI, High CBT	Thaumarchaeota and Euryarchaeota produced in soil	Soil bacteria
The Yukon–Tanana River	Sand and silt	Low isoprenoid and high branched GDGT concentrations, High BIT, High TEX_{86} and TEX^{L}_{86}, High Cald/Cren, High MI, High CBT	Thaumarchaeota and Euryarchaeota produced in soil	Soil bacteria
The Mackenzie River estuary	Sand and silt	Low isoprenoid and high branched GDGT concentrations, High BIT, Moderate TEX_{86} and TEX^{L}_{86}, High Cald/Cren, High MI, High CBT	Thaumarchaeota and Euryarchaeota produced in soil	Soil bacteria

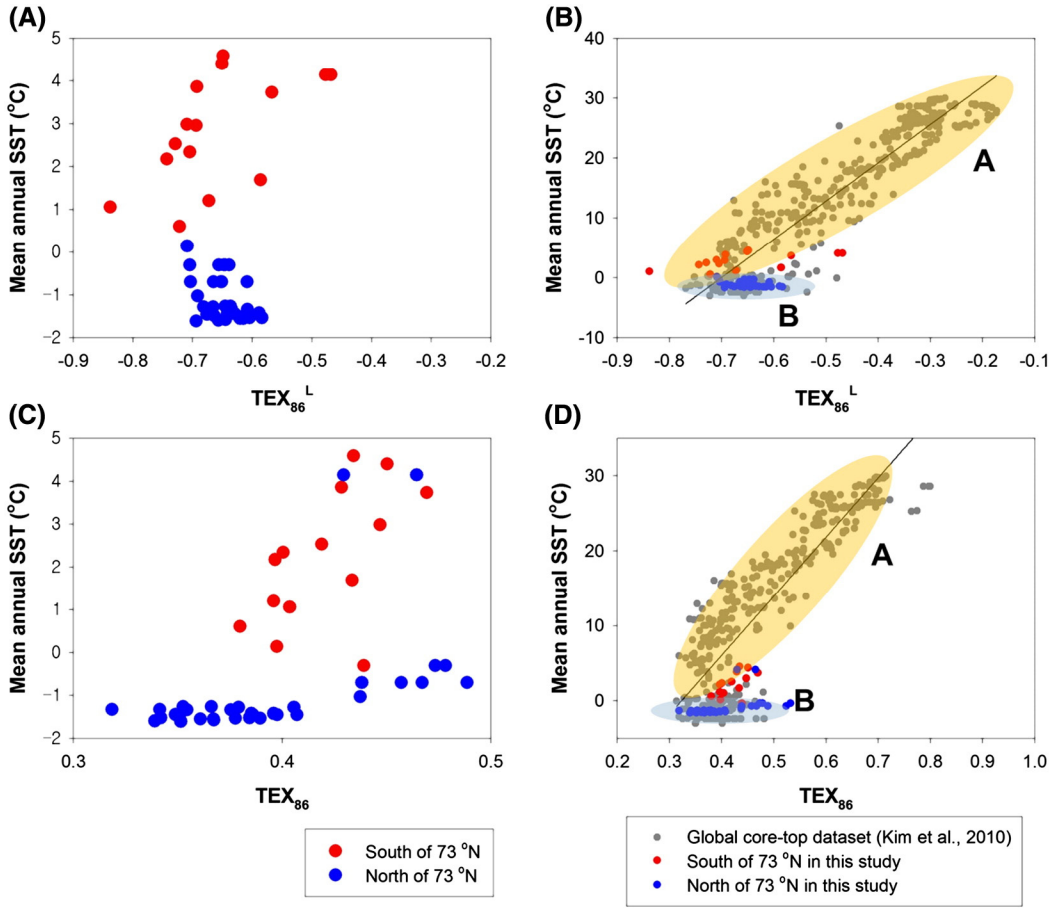

Fig. 6. TEX_{86} and TEX_{86}^{L} against mean annual SST in the studied samples compared to the global core-top dataset (Kim et al., 2010). The regression line in panels (B) and (D) refers to the global core-top dataset (Kim et al., 2010).

5.3. TEX_{86} thermometry

The comparison of TEX_{86}- and TEX_{86}^{L}-derived temperatures with climatological SSTs shows various patterns in the study areas (Fig. 5). The anomalously high TEX_{86}- and TEX_{86}^{L}-derived temperatures in the Yukon River estuary (7.3–24.4 °C) likely reflect the isoprenoid GDGT composition derived from the river (11.3–24.7 °C; Figs. 4L and 5). In other areas, the TEX_{86}- and TEX_{86}^{L}-derived values are closer to the annual ranges of SSTs south of the shelf edge around 73 °N and higher further north (Figs. 5, 6A and C). The southern group of samples shows a positive

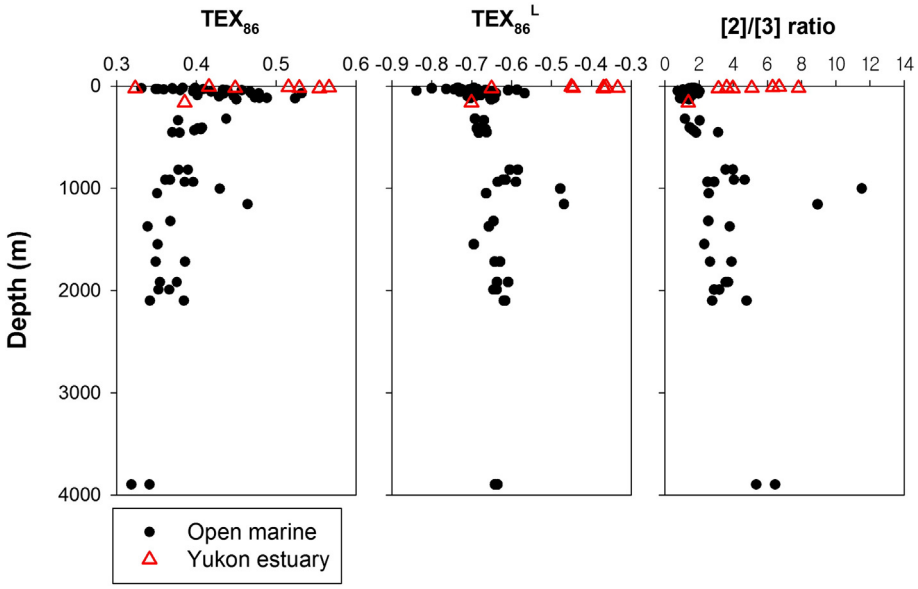

Fig. 7. Depth profiles of TEX_{86}, TEX_{86}^{L} and the ratio of GDGT-2 to GDGT-3 in open marine sediments.

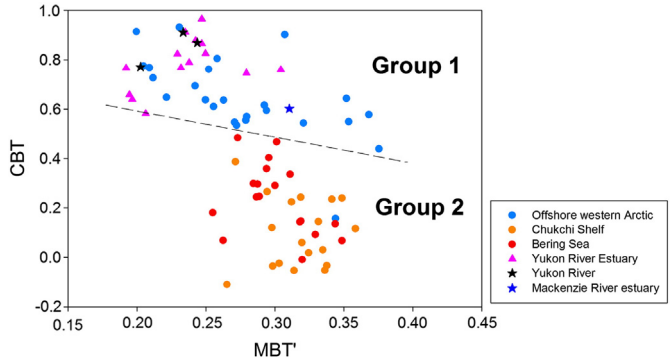

Fig. 8. CBT vs MBT′ values in surface sediments from the western Arctic Ocean, the Chukchi Sea, Bering Sea, the Yukon and Mackenzie River estuaries, and the Yukon River sediments.

correlation between TEX_{86} and SST ($r = 0.79$, $n = 14$, $p < 0.01$) and between TEX_{86}^{L} and SST ($r = 0.60$, $n = 14$, $p < 0.05$), and they are consistent with group A of the global core-top dataset of Kim et al. (2010) (Fig. 6B and D). The group of samples north of 73 °N shows a wide range of TEX_{86} and TEX_{86}^{L} in a narrow SST interval around −1 °C (Fig. 6A and C), which is consistent with group B of the global core-top dataset of Kim et al. (2010) (Fig. 6B and D).

One may consider that the advection of isoprenoid GDGTs from the Bering and southern Chukchi Seas influences TEX_{86}- and TEX_{86}^{L}-derived temperatures in the area north of 73 °N. The contribution of terrestrial soils may also affect the TEX_{86} and TEX_{86}^{L} distribution as sediments in the Yukon River have high TEX_{86}- and TEX_{86}^{L}-values (Figs. 4K and 5). However, the Cald/Cren ratio and MI in the northern samples are more similar to these indices on the inner shelf of the Chukchi Sea rather than the Yukon River sediments (Fig. 4G and I), indicating that the influence of terrestrial GDGTs on TEX_{86} and TEX_{86}^{L} in the study area is negligible. The CBT values of branched GDGTs in the northern group are also different from the southern group (Fig. 4M and O), suggesting a limited influence of GDGTs transported from southern areas on TEX_{86} and TEX_{86}^{L} further north. It is also less likely that the degradation of GDGTs affected TEX_{86} and TEX_{86}^{L} because field experiment, sediment trap and surface sediment studies showed no significant change in TEX_{86} and TEX_{86}^{L} during oxic degradation (Kim et al., 2009; Yamamoto et al., 2012). Recent core-top studies in the Mediterranean Sea and the South China Sea indicate TEX_{86} values in deep water sites are significantly higher than those in the adjacent shallow sites (Ge et al., 2013; Leider et al., 2010). The depth plots of TEX_{86} and TEX_{86}^{L} in open marine sediments do not show such trend, although the ratio of GDGT-2 to GDGT-3 increases with increasing water depth (Fig. 7), as also reported global ocean sediments by Taylor et al. (2013).

The question, why TEX_{86}- and TEX_{86}^{L}-derived temperatures are higher than SST in the area north of 73 °N, remains open. One explanation can be offered by recent studies on intact GDGTs in suspended particulates suggesting that the response of TEX_{86} to temperature is affected by epipelagic or mesopelagic Thaumarchaeotal communities (Chun Zhu, personal communication). We speculate that such difference in Thaumarchaeotal communities might influence the spatial distribution of TEX_{86} and TEX_{86}^{L} in the study area as well (Table 1).

5.4. Sources of branched GDGTs in the western Arctic

High concentrations of branched GDGTs in sediments from estuaries of the Yukon and Mackenzie rivers, which contain the highest suspended matter loads in the Arctic (Macdonald et al., 2004), are attributed to the discharge of soil organic matter. In the Yukon River estuary, branched GDGT concentrations remarkably decrease with distance from the river mouth, suggesting that a large fraction of soil organic matter is deposited in the river proximity. At the shelf edge of the Chukchi Sea, both branched and isoprenoid GDGTs are abundant, indicating common depositional processes such as sediment resuspension and redeposition and efficient preservation in sediment depocenters.

Spatial distribution of the BIT index is consistent with that of branched GDGT concentrations (Fig. 4C and E). High values appeared in the Yukon River and Mackenzie River estuaries (Fig. 4E and F). Exceptionally, relatively high BIT (0.23 to 0.39) co-occurs with low branched GDGT concentration at some sites north of 75 °N (Fig. 5). There are two possible interpretations of this phenomenon. First, low Thaumarchaeota production under the perennial sea ice resulted in low crenarchaeol concentration and thus higher BIT. Second, the GDGTs in this area are expected to suffer severe degradation due to the oxic conditions and low sedimentation rates (e.g., Polyak et al., 2009). Huguet et al. (2009) showed that the BIT values in oxic sediment layers were higher than in anoxic layers as exemplified by turbidites from the Madeira Abyssal Plain (Huguet et al., 2009). Estimates of the first-order decomposition rate constants for isoprenoid GDGTs (2.5×10^{-5} yr^{-1}) and branched GDGTs (2.0×10^{-5} yr^{-1}) in a sediment core from the Arctic Ocean (Yamamoto and Polyak, 2009) indicate that branched GDGTs are more refractory than isoprenoid GDGTs. This result is consistent with a combined study of sediment trap and underlying sediment showing that preservation rates are higher for branched GDGTs than isoprenoid GDGTs at the water-sediment interface (Yamamoto et al., 2013). This difference in preservation rates potentially affects the distribution of BIT values in marine sediments. It is, thus, likely that relatively high BIT in the area north of 75 °N is biased by the selective degradation of isoprenoid GDGTs as compared with branched GDGTs.

Two groups of branched GDGTs in the studied sediments are illustrated by the diagram of CBT vs MBT′ (Fig. 8). The first group, characterized by high CBT values, consists of samples from the Arctic Ocean north of 75 °N, the Yukon and Mackenzie River estuaries, and Yukon–Tanana River sediments (Group 1 in Fig. 8). The second group, low-CBT group comprises samples from the Chukchi and Bering Seas (Group 2 in Fig. 8). In Group 1, MBT′/CBT-based temperatures (ca. 0 °C) are higher than the MAATs at Barrow (−11 °C) and Nome (−3 °C) in northern Alaska, and the CBT-based pH values (6.5) are similar to the measured soil pH values in Alaskan soils (3.6–7.7 [Yu-Hyeon Park, unpublished data]). In contrast, in Group 2, MBT′/CBT-base temperatures (ca. 7 °C) are much higher than the MAATs in northern Alaska, and the CBT-based pH values are also higher than those in Alaskan soils. Weijers et al. (2011) reported that MBT/CBT overestimated temperature and pH in a peat sequence in Switzerland and pointed out that this index is sensitive to changes in vegetation. This result suggests a possibility that the GDGT composition difference between the two groups of samples in our study may reflect a difference in vegetation of the provenance areas. However, a preliminary analysis of 47 peat and soil samples at 17 different sites in tundra and taiga vegetation in Alaska indicates predominantly high CBT values (Yu-Hyeon Park, unpublished data), which are consistent with values in the Group 1. Although we do not have data for Siberian peats and soils, this preliminary result suggests that vegetation is not a key factor differentiating CBT values. Peterse et al. (2009) and Zhu et al. (2011) found lower CBT and higher MBT in marine surface sediments than in coastal soils and suggested in situ production of branched GDGTs in marine environments. Zell et al. (2014) reported the same phenomenon for the Amazon River estuary. We suppose that the branched GDGTs in Group 2 (Chukchi shelf and the Bering Sea samples) were derived from marine bacteria. On the other hands, in the western Arctic Ocean north of 75 °N, branched GDGTs with higher CBT were possibly derived from terrestrial soil organic matter (Table 1). In the Yukon River estuary, the sediments at proximal sites have higher CBT, corresponding to the values of Yukon River sediments (group 1), than the sediments at distal sites (group 2) (Fig. 4N). The seaward decrease of CBT values reflects the increasing contribution of branched GDGTs of marine origin (Table 1).

6. Conclusions

A relatively high abundance of isoprenoid GDGTs on the outer shelf and slope of the Chukchi Sea and the upper slope of the Bering Sea are attributed to a combination of higher production of Thaumarchaeota at the shelf edge, redeposition of GDGT-enriched fine particles, and better preservation of GDGTs due to higher sedimentation rate by sediment focusing. The TEX_{86}- and TEX_{86}^{L}-derived temperatures in samples north of 73 °N are unrealistically high as compared to SSTs. This bias might be attributed to different Thaumarchaeotal communities in this area. TEX_{86}- and TEX_{86}^{L}-derived temperatures further south compare better with the global SST core-top calibration, but their applicability for paleothermometry yet needs to be evaluated. Branched GDGTs are abundant in the Yukon and Mackenzie River estuaries and on the inner and outer shelf of the Chukchi Sea. Sediments from the western Arctic Ocean north of 75 °N, the Yukon and Mackenzie River estuaries, and the Yukon–Tanana River have higher CBT than sediments from the Chukchi and Bering Seas. The temperatures and pH values (ca. 0–1 °C and 6.5, respectively) estimated by MBT′/CBT in the western Arctic Ocean north of 75 °N are representative for Arctic terrestrial environments. In the Chukchi and Bering Sea sediments these values are ca. 7 °C and 8.5, respectively, much higher than those in Alaska soil. This pattern suggests two different sources of branched GDGTs, which we tentatively attribute to soil and in situ marine bacteria, respectively.

Acknowledgments

We thank all of the captain, crew and scientists of RV Araon, RV Mirai, T/S Oshoro-maru and IB USCGC Healy for their help during the cruise of sampling. We also thank K. Ohnishi of Hokkaido University for analytical assistance and Dr. S. Yoon of Hokkaido University for comment of scientific visualization. Comments by Prof. F. J. Millero and two anonymous reviewers improved this manuscript. The study was supported by a grant-in-aid for Scientific Research (A) from the Japan Society for the Promotion of Science, No. 25287136 (to M.Y.), K-Polar Program (PP13030) and Basic Research Program (PE14062) of Korea Polar Research Institute (to SIN), and the Polar Academic Program (to BKK).

Appendix A. Structures of isoprenoid and branched glycerol dialkyl glycerol tetraethers

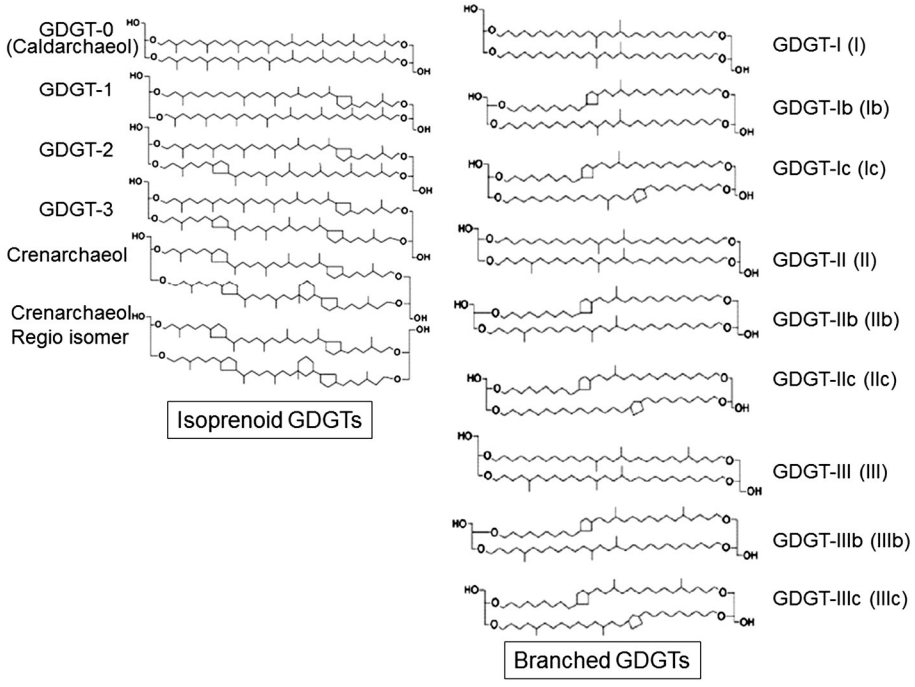

References

Agogué, H., Brink, M., Dinasquet, J., Herndl, G.J., 2008. Major gradients in putatively nitrifying and non-nitrifying Archaea in the deep North Atlantic. Nature 456, 788–792.

Alonso-Sáez, L., Sánchez, O., Gasol, J.M., Balagué, V., Pedrós-Alio, C., 2008. Winter-to-summer changes in the composition and single-cell activity of near-surface Arctic prokaryotes. Environ. Microbiol. 10, 2444–2454.

Alonso-Sáez, L., Waller, A.S., Mende, D.R., Bakker, K., Farnelid, H., Yager, P.L., Lovejoy, C., Tremblay, J.-É., Potvin, M., Heinrich, F., Estrada, M., Riemann, L., Bork, P., Pedrós-Alió, C., Bertilsson, S., 2012. Role for urea in nitrification by polar marine Archaea. Proc. Natl. Acad. Sci. 109, 17989–17994.

Amano-Sato, C., Akiyama, S., Uchida, M., Shimada, K., Utsumi, M., 2013. Archaeal distribution and abundance in water masses of the Arctic Ocean, Pacific sector. Aquat. Microb. Ecol. 69, 101–112.

Are, F.E., 1996. Dynamics of the littoral zone of Arctic Seas (state of the art and goals). Polarforschung 64, 123–131.

Arrigo, K.R., van Dijken, G., Pabi, S., 2008. Impact of a shrinking Arctic ice cover on marine primary production. Geophys. Res. Lett. 35, L19603. http://dx.doi.org/10.1029/2008GL035028.

Bano, N., Ruffin, S., Ransom, B., Hollibaugh, J.T., 2004. Phylogenetic composition of Arctic Ocean archaeal assemblages and comparison with Antarctic assemblages. Appl. Environ. Microbiol. 70, 781–789.

Bates, N.R., Cai, W.-J., Mathis, J.T., 2011. The ocean carbon cycle in the western Arctic Ocean: distributions and air–sea fluxes of carbon dioxide. Oceanography 24, 186–201.

Belicka, L.L., Harvey, H.R., 2009. The sequestration of terrestrial organic carbon in Arctic Ocean sediments: a comparison of methods and implications for regional carbon budgets. Geochim. Cosmochim. Acta 73, 6231–6248.

Belicka, L.L., MacDonald, R.W., Harvey, H.R., 2002. Sources and transport of organic carbon to shelf, slope, and basin surface sediments of the Arctic Ocean. Deep-Sea Res. I 49, 1463–1483.

Blaga, C.I., Reichart, G.J., Heiri, O., Sinninghe Damsté, J.S., 2009. Tetraether membrane lipid distributions in lake particulate matter and sediments: a study of 47 European lakes along a North–South transect. J. Paleolimnol. 41, 523–540.

Brabets, T.P., Wang, B., Meade, R.H., 2000. Environmental and hydrologic overview of the Yukon River Basin, Alaska and Canada. U.S. Geological Survey Water-Resources Investigations Report 99-4204 (106 pp.).

Codispoti, L.A., Flagg, C., Kelly, V., Swift, J.H., 2005. Hydrographic conditions during the 2002 SBI process experiments. Deep-Sea Res. II 52, 3199–3226.

Cota, G.F., Pomeroy, L.R., Harrison, W.G., Jones, E.P., Peters, F., Sheldon, W.M., Weingartner, T.R., 1996. Nutrients, primary production and microbial heterotrophy in the southeastern Chukchi Sea: Arctic summer nutrient depletion and heterotrophy. Mar. Ecol. Prog. Ser. 135, 247–258.

Darby, D.A., 2003. Sources of sediment found in sea ice from the western Arctic Ocean, new insights into processes of entrainment and drift patterns. J. Geophys. Res. 108 (C8), 3257. http://dx.doi.org/10.1029/2002JC001350.

Darby, D.A., Ortiz, J.D., Polyak, L., Lund, S., Jakobsson, M., Woodgate, R.A., 2009. The role of currents and sea ice in both slowly deposited central Arctic and rapidly deposited Chukchi–Alaskan margin sediments. Glob. Planet. Chang. 68, 58–72.

DeLong, E.F., Wu, K.Y., Prezelin, B.B., Jovine, R.V., 1994. High abundance of Archaea in Antarctic marine picoplankton. Nature 371, 695–697.

Faux, J.F., Belicka, L.L., Harvey, H.R., 2011. Organic sources and carbon sequestration in Holocene shelf sediments from the western Arctic Ocean. Cont. Shelf Res. 31, 1169–1179.

Ge, H., Zhang, C., Dang, H., Zhu, C., Jia, G., 2013. Distribution of tetraether lipids in surface sediments of the northern South China Sea: implications for TEX86 proxies. Geosci. Front. 4, 223–229.

Giles, K.A., Laxon, S.W., Ridout, A.L., Wingham, D.J., Bacon, S., 2012. Western Arctic Ocean freshwater storage increased by wind-driven spin-up of the Beaufort Gyre. Nat. Geosci. 5, 194–197.

Gordeev, V.V., 2006. Fluvial sediment flux to the Arctic Ocean. Geomorphology 80, 94–104.

Grebmeier, J.M., Cooper, L.W., Feder, H.M., Sirenko, B.I., 2006. Ecosystem dynamics of the Pacific-influenced northern Bering and Chukchi Seas. Prog. Oceanogr. 71, 331–361.

Hallam, S.J., Mincer, T.J., Schleper, C., Preston, C.M., Roberts, K., Richardson, P.M., DeLong, E.F., 2006. Pathway of carbon assimilation and ammonia oxidation suggested by environmental genomic analyses of marine Crenarchaeota. PLoS Biol. 4, 520–536.

Harper, J.R., 1978. Coastal erosion rates along the Chukchi Sea coast near Barrow, Alaska. Arctic 31, 428–433.

Hill, V.J., Cota, G.F., 2005. Spatial patterns of primary production, in the Chukchi Sea in the spring and summer of 2002. Deep-Sea Res. II 52, 3344–3354.

Ho, S.L., Mollenhauer, G., Fietz, S., Martínez-Garcia, A., Lamy, F., Rueda, G., Schipper, K., Mehéust, M., Rosell-Melé, A., Stein, R., Tiedemann, R., 2014. Appraisal of TEX_{86} and TEX^{L}_{86} thermometries in subpolar and polar regions. Geochim. Cosmochim. Acta 131, 213–226.

Holmes, R.M., McClelland, J.W., Peterson, B., Shiklomanov, I.A., Shiklomanov, A.I., Zhulidov, A.V., Gordeev, V.V., Bobrovitskaya, N.N., 2002. A circumpolar perspective on fluvial sediment flux to the Arctic Ocean. Glob. Biogeochem. Cycles 16, 1098. http://dx.doi.org/10.1029/2001GB001849.

Hopmans, E.C., Schouten, S., Pancost, R.D., van der Meer, M.T.J., Sinninghe Damsté, J.S., 2000. Analysis of intact tetraether lipids in archaeal cell material and sediments by high performance liquid chromatography/atmospheric pressure chemical ionization mass spectrometry. Rapid Commun. Mass Spectrom. 14, 585–589.

Hopmans, E.C., Weijers, J.W.H., Schefuss, E., Herfort, L., Sinninghe Damsté, J.S., Schouten, S., 2004. A novel proxy for terrestrial organic matter in sediments based on branched and isoprenoid tetraether lipids. Earth Planet. Sci. Lett. 24, 107–116.

Huguet, C., Hopmans, E.C., Febo-Ayala, W., Thompson, D.H., Sinninghe Damsté, J.S.S., Schouten, S., 2006. An improved method to determine the absolute abundance of glycerol dibiphytanyl glycerol tetraether lipids. Org. Geochem. 37, 1036–1041.

Huguet, C., Kim, J.-H., de Lange, G.J., Sinninghe Damsté, J.S., Schouten, S., 2009. Effects of long term oxic degradation on the $U^{K'}_{37}$, TEX_{86} and BIT organic proxies. Org. Geochem. 40, 1188–1194.

Kalinenko, V.V., 2001. Clay minerals in sediments of the Arctic Seas. Lithol. Miner. Resour. 36, 362–372 (Translated from Litologiya I Poleznye Iskopaemye 4, 418–429).

Kim, J.-H., Huguet, C., Zonneveld, K.A., Versteegh, G.J., Roeder, W., Sinninghe Damsté, J.S., Schouten, S., 2009. An experimental field study to test the stability of lipids used for the TEX_{86} and palaeothermometers. Geochim. Cosmochim. Acta 73, 2888–2898.

Kim, J.-H., van der Meer, J., Schouten, S., Helmke, P., Willmott, V., Sangiorgi, F., Koc, N., Hopmans, E.C., Sinninghe Damsté, J.S., 2010. New indices and calibrations derived from the distribution of crenarchaeal isoprenoid tetraether lipids: implications for past sea surface temperature reconstructions. Geochim. Cosmochim. Acta 74, 4639–4654.

Kim, J.-H., Crosta, X., Willmott, V., Renssen, H., Bonnin, J., Helmke, P., Schouten, S., Sinninghe Damsté, J.S., 2012. Holocene subsurface temperature variability in the eastern Antarctic continental margin. Geophys. Res. Lett. 39, L06705. http://dx.doi.org/10.1029/2012GL051157.

Kirchman, D.L., Elifantz, H., Dittel, A.I., Malmstrom, R.R., Cottrell, M.T., 2007. Standing stocks and activity of Archaea and bacteria in the western Arctic Ocean. Limnol. Oceanogr. 52, 495–507.

Könneke, M., Bernhard, A.E., de la Torre, J.R., Walker, C.B., Waterbury, J.B., Stahl, D.A., 2005. Isolation of an autotrophic ammonia-oxidizing marine archaeon. Nature 437, 543–546.

Lee, S.H., Stockwell, D., Whitledge, T.E., 2010. Uptake rates of dissolved inorganic carbon and nitrogen by under-ice phytoplankton in the Canada Basin in summer 2005. Polar Biol. 33, 1027–1036.

Leider, A., Hinrichs, K.U., Mollenhauer, G., Versteegh, G.J., 2010. Core-top calibration of the lipid-based $U^{K}_{37'}$ and TEX_{86} temperature proxies on the southern Italian shelf (SW Adriatic Sea, Gulf of Taranto). Earth Planet. Sci. Lett. 300, 112–124.

Liu, Z., Pagani, M., Zinniker, D., DeConto, R., Huber, M., Brinkhuis, H., Shah, S., Leckie, R.M., Pearson, A., 2009. Global cooling during the Eocene–Oligocene climate transition. Science 323, 1187–1190.

Macdonald, R.W., McLaughlin, F.A., Carmack, E.C., 2002. Fresh water and its sources during the SHEBA drift in the Canada Basin of the Arctic Ocean. Deep-Sea Res. I 49, 1769–1785. http://dx.doi.org/10.1016/S0967-0637(02)00097-3.

Macdonald, R.W., Naidu, A.S., Yunker, M.B., Gobeil, C., 2004. The Beaufort Sea: distribution, sources, fluxes, and burial of organic carbon. In: Stein, R., Macdonald, R.W. (Eds.), The Organic Carbon Cycle in the Arctic Ocean. Springer-Verlag.

Miller, G.H., Alley, E.B., Brigham-Grette, J., Fitzpatrick, J.J., Polyak, L., Serreze, M.C., White, J.W.C., 2010. Arctic amplification: can the past constrain the future? Quat. Sci. Rev. 29, 1779–1790.

Nagashima, K., Asahara, Y., Takeuchi, F., Harada, N., Toyoda, S., Tada, R., 2012. Contribution of detrital materials from the Yukon River to the continental shelf sediments of the Bering Sea based on the electron spin resonance signal intensity and crystallinity of quartz. Deep-Sea Res. II 61, 145–154.

Nishihara, M., Koga, Y., 1987. Extraction and composition of polar lipids from the archaebacterium, *Methanobacterium thermoautotrophicum*: effective extraction of tetraether lipids by an acidified solvent. J. Biochem. 101, 997–1005.

Ortiz, J.D., Orsburn, C., Polyak, L., Grebmeier, J.M., Darby, D.A., Eberl, D.D., Naidu, S., Nof, D., 2009. Provenance of Holocene sediment on the Chukchi Shelf–Alaskan margin based on combined diffuse spectral reflectance and quantitative X-ray diffraction analysis. Glob. Planet. Chang. 68, 73–84.

Ouverney, C.C., Fuhrman, J.A., 2000. Marine planktonic Archaea take up amino-acids. Appl. Environ. Microbiol. 66, 4829–4833.

Patwardhan, A.P., Thompson, D.H., 1999. Efficient synthesis of 40-and 48-membered tetraether macrocyclic bisphosphocholines. Org. Lett. 1, 241–244.

Peterse, F., Kim, J.-H., Schouten, S., Kristensen, D.K., Koc, Sinninghe Damsté, J.S., 2009. Constraints on the application of the MBT/CBT palaeothermometry at high latitude environments. Org. Geochem. 40, 692–699.

Peterse, F., Meer, J.V.D., Schouten, S., Weijers, J.W.H., Fierer, N., Jackson, R.B., Kim, J.-H., Sinninghe Damsté, J.S., 2012. Revised calibration of the MBT–CBT paleotemperature proxy based on branched tetraether membrane lipids in surface soils. Geochim. Cosmochim. Acta 96, 215–229.

Pickart, R.S., 2004. Shelfbreak circulation in the Alaskan Beaufort Sea: mean structure and variability. J. Geophys. Res. 109, C04024. http://dx.doi.org/10.1029/2003JC001912.

Pickart, R.S., Weingartner, T.J., Pratt, L.J., Zimmermann, S., Torres, D.J., 2005. Flow of winter-transformed Pacific water into the Western Arctic. Deep-Sea Res. II 52, 3175–3198.

Polyak, L., Bischof, J., Ortiz, J., Darby, D., Channell, J., Xuan, C., Kaufman, D., Lovlie, R., Schneider, D., Adler, R., 2009. Late Quaternary stratigraphy and sedimentation patterns in the western Arctic Ocean. Glob. Planet. Chang. 68, 5–17.

Polyak, L., Alley, R.B., Andrews, J.T., Brigham-Grette, J., Cronin, T.M., Darby, D.A., Dyke, A.S., Fitzpatrick, J.J., Funder, S., Holland, M., Jennings, A.E., Miller, G.H., O'Regan, M., Savelle, J., Serreze, M., St. John, K., White, J.W.C., Wolff, E., 2010. History of sea ice in the Arctic. Quat. Sci. Rev. 29, 1757–1778.

Schouten, S., Hopmans, E.C., Schefuß, E., Sinninghe Damsté, J.S., 2002. Distributional variations in marine crenarchaeotal membrane lipids: a new tool for reconstructing ancient sea water temperatures? Earth Planet. Sci. Lett. 204, 265–274.

Schouten, S., Huguet, C., Hopmans, E.C., Kienhuis, M.V.M., Sinninghe Damsté, J.S., 2007. Analytical methodology for TEX_{86} paleothermometry by high performance liquid chromatography/atmospheric pressure chemical ionization-mass spectrometry. Anal. Chem. 79, 2940–2944.

Schouten, S., Hopmans, E.C., Sinninghe Damsté, J.S., 2013. The organic geochemistry of glycerol dialkyl glycerol tetraether lipids: a review. Org. Geochem. 54, 19–61.

Screen, J.A., Simmonds, I., 2010. The central role of diminishing sea ice in recent Arctic temperature amplification. Nature 464, 1334–1337.

Shimada, K., Kamoshida, T., Itoh, M., Nishino, S., Carmack, E., McLaughlin, F., Zimmermann, S., Proshutinsky, A., 2006. Pacific Ocean inflow: influence on catastrophic reduction of sea ice cover in the Arctic Ocean. Geophys. Res. Lett. 33, L08605. http://dx.doi.org/10.1029/2005GL025624.

Sinninghe Damsté, J.S., Hopmans, E.C., Pancost, R.D., Schouten, S., Geenevasen, J.A.J., 2000. Newly discovered non-isoprenoid dialkyl diglycerol tetraether lipids in sediments. Chem. Commun. 23, 1683–1684.

Sinninghe Damsté, J.S., Schouten, S., Hopmans, E.C., van Duin, A.C.T., Geenevasen, J.A.J., 2002. Crenarchaeol: the characteristic core glycerol dibiphytanyl glycerol tetraether membrane lipid of cosmopolitan pelagic crenarchaeota. J. Lipid Res. 43, 1641–1651.

Sinninghe Damsté, J.S., Ossebaar, J., Abbas, B., Schouten, S., Verschuren, D., 2009. Fluxes and distribution of tetraether lipids in an equatorial African lake: constraints on the application of the TEX_{86} palaeothermometer and branched tetraether lipids in lacustrine settings. Geochim. Cosmochim. Acta 73, 4232–4249.

Sinninghe Damsté, J.S., Rijpstra, W.I.C., Hopmans, E.C., Weijers, J.W.H., Foesel, B.U., Overmann, J., Dedysh, S.N., 2011. 13,16-Dimethyl octacosanedioic acid (iso-diabolic acid): a common membrane-spanning lipid of Acidobacteria subdivisions 1 and 3. Appl. Environ. Microbiol. 77, 4147–4154.

Spang, A., Hatzenpichler, R., Brochier-Armanet, C., Rattei, T., Tischler, P., Spieck, E., Streit, W., Stahl, D.A., Wagner, M., Schleper, C., 2010. Distinct gene set in two different lineages of ammonia-oxidizing archaeal supports the phylum Thaumarchaeota. Trends Microbiol. 18, 331–340.

Stein, R., Grobe, H., Wahsner, M., 1994. Organic carbon, carbonate, and clay mineral distributions in eastern central Arctic Ocean surface sediments. Mar. Geol. 119, 269–285.

Stein, R., Dittmers, K.H., Fahl, K., Kraus, M., Matthiessen, J., Niessen, F., Pirrung, M., Polyakova, Y.I., Schoster, F., Steinke, T., Fütterer, D.K., 2004. Arctic (palaeo) river

discharge and environmental change: evidence from the Holocene Kara Sea sedimentary record. Quat. Sci. Rev. 23, 1485–1511.
Taylor, K.W., Huber, M., Hollis, C.J., Hernandez-Sanchez, M.T., Pancost, R.D., 2013. Re-evaluating modern and Palaeogene GDGT distributions: implications for SST reconstructions. Glob. Planet. Chang. 108, 158–174.
Tierney, J.E., Russell, J.M., 2009. Distributions of branched GDGTs in a tropical lake system: implications for lacustrine application of the MBT/CBT paleoproxy. Org. Geochem. 40, 1032–1036.
Viscosi-Shirley, C., Pisias, N., Mammone, K., 2003. Sediment source strength, transport pathways and accumulation patterns on the Siberian–Arctic's Chukchi and Laptev shelves. Cont. Shelf Res. 23, 1201–1225.
Wang, J., Cota, G.F., Comiso, J.C., 2005. Phytoplankton in the Beaufort and Chukchi Seas: distribution, dynamics, and environmental forcing. Deep-Sea Res. II 52, 3355–3368.
Weijers, J.W.H., Schouten, S., van Den Donker, J.C., Hopmans, E.C., Sinninghe Damsté, J.S., 2007. Environmental controls on bacterial tetraether membrane lipid distribution in soils. Geochim. Cosmochim. Acta 71, 703–713.
Weijers, J.W.H., Steinmann, P.S., Hopmans, E.C., Schouten, S., Sinninghe Damsté, J.S., 2011. Bacterial tetraether membrane lipids in peat and coal: testing the MBT–CBT temperature proxy for climate reconstruction. Org. Geochem. 42, 477–486.
Weingartner, T., Aagaard, K., Woodgate, R., Danielson, S., Sasaki, Y., Cavalieri, D., 2005. Circulation on the north central Chukchi Sea shelf. Deep-Sea Res. II 52, 3150–3174.
Williams, W.J., Melling, H., Carmack, E.C., Ingram, R.G., 2008. Kugmallit Valley as a conduit for cross-shelf exchange on the Mackenzie Shelf in the Beaufort Sea. J. Geophys. Res. 113, C02007. http://dx.doi.org/10.1029/2006JC003591.
Woodgate, R.A., Aagaard, K., 2005. Revising the Bering Strait freshwater flux into the Arctic Ocean. Geophys. Res. Lett. 32, L02602. http://dx.doi.org/10.1029/2004GL021747.
Woodgate, R.A., Aagaard, K., Swift, J.H., Falkner, K.K., Smethie, W.M., 2005a. Pacific ventilation of the Arctic Ocean's lower halocline by upwelling and diapycnal mixing over the continental margin. Geophys. Res. Lett. 32, L18609. http://dx.doi.org/10.1029/2005GL023999.
Woodgate, R.A., Aagaard, K., Weingartner, T., 2005b. A year in the physical oceanography of the Chukchi Sea: moored measurements from autumn 1990–1991. Deep-Sea Res. II 52, 3116–3149.
Wuchter, C., Abbas, B., Coolen, M.J.L., Herfort, L., Timmers, P., Strous, M., van Bleijswijk, J., Teira, E., Herndl, G.J., Middelburg, J.J., Schouten, S., Sinninghe Damsté, J.S., 2006. Archaeal nitrification in the ocean. Proc. Natl. Acad. Sci. U. S. A. 103, 12317–12322.
Yamamoto, M., Polyak, L., 2009. Changes in terrestrial organic matter input to the Mendeleev Ridge, western Arctic Ocean, during the Late Quaternary. Glob. Planet. Chang. 68, 30–37.
Yamamoto, M., Okino, T., Sugisaki, S., Sakamoto, T., 2008. Late Pleistocene changes in terrestrial biomarkers in sediments from the central Arctic Ocean. Org. Geochem. 39, 754–763.
Yamamoto, M., Shimamoto, A., Fukuhara, T., Tanaka, Y., 2013. Branched glycerol dialkyl glycerol tetraethers in sinking particles in the western North Pacific. Book of abstract of the 26th IMOG, p. 121.
Yamamoto, M., Shimamoto, A., Fukuhara, T., Tanaka, Y., Ishizaka, J., 2012. Glycerol dialkyl glycerol tetraethers and TEX_{86} index in sinking particles in the western North Pacific. Org. Geochem. 53, 52–62.
Yunker, M.B., Macdonald, R.W., Cretney, W.J., Fowler, B.R., McLaughlin, F.A., 1993. Alkane, terpene, and polycyclic aromatic hydrocarbon geochemistry of the Mackenzie River and Mackenzie shelf: riverine contributions to Beaufort Sea coastal sediment. Geochim. Cosmochim. Acta 57, 3041–3061.
Yunker, M.B., Macdonald, R.W., Snowdon, L.R., Fowler, B.R., 2011. Alkane and PAH biomarkers as tracers of terrigenous organic carbon in Arctic Ocean sediments. Org. Geochem. 42, 1109–1146.
Yurco, L.N., Ortiz, J.D., Polyak, L., Darby, D.A., Crawford, K.A., 2010. Clay mineral cycles identified by diffuse spectral reflectance in Quaternary sediments from the Northwind Ridge: implications for glacial–interglacial sedimentation patterns in the Arctic Ocean. Polar Res. 29, 176–197.
Zell, C., Kim, J.-H., Hollander, D., Lorenzoni, L., Baker, P., Silva, C.G., Nittrouer, C., Sinninghe Damsté, J.S., 2014. Sources and distributions of branched and isoprenoid tetraether lipids on the Amazon shelf and fan: implications for the use of GDGT-based proxies in marine sediments. Geochim. Cosmochim. Acta 139, 293–312.
Zhang, Y., Sintes, E., Chen, J., Zhang, Y., Dai, M., Jiao, N., Herndl, G.J., 2009. Role of mesoscale cyclonic eddies in the distribution and activity of Archaea and Bacteria in the South China Sea. Aquat. Microb. Ecol. 56, 65–79.
Zhang, Y.G., Zhang, C., Liu, X.-I., Li, L., Hinrichs, K.U., Noakes, J.E., 2011. Methane index: a tetraether archaeal lipid biomarker indicator for detecting the instability of marine gas hydrates. Earth Planet. Sci. Lett. 307, 525–534.
Zhu, C., Weijers, J.W.H., Wagner, T., Pan, J.M., Chen, J.F., Pancost, R.D., 2011. Sources and distributions of tetraether lipids in surface sediments across a large river-dominated continental margin. Org. Geochem. 42, 376–386.